

Lateral Spreading in Christchurch, New Zealand: An Empirical Approach

Megah Ultari

Department of Civil Engineering, Faculty of Civil and Environmental Engineering,
Institut Teknologi Bandung, Indonesia

*Corresponding author, e-mail: Megaulta@yahoo.com

Received 28th July 2024; Revision 29th August 2024; Accepted 23th September 2024

ABSTRACT

Lateral spreading, a complex phenomenon resulting from liquefaction, manifests when saturated, cohesionless soils lose their strength during seismic events, causing them to deform and flow horizontally. This process poses a substantial risk to buildings and infrastructure, often resulting in extensive damage, significant financial burdens, and, tragically, loss of life. In Indonesian, liquefaction is recognized for its ability to transform solid ground into a fluid-like state, amplifying its danger in regions prone to earthquakes. This study aims to analyze lateral spreading through empirical methods, specifically employing the Bartlett & Youd Method (2002) and the Byrne Method (1990). The analysis focuses on sites previously affected by lateral spreading, notably those impacted by the 22 February 2011 Christchurch earthquake, which registered a magnitude of 6.2 and a peak ground acceleration of 0.52. The selected locations include the South Brighton Bridge, Anzac Bridge, and Fitzgerald Bridge in Christchurch, New Zealand. The findings demonstrate that both the Bartlett & Youd Method (2002) and the Byrne Method (1990) yield results that closely approximate the actual conditions at site.

Keywords: *Lateral Spreading; Empirical Method; Bartlett & Youd Method (2002); Byrne Method (1990).*

Copyright © Megah Ultari

This is an open-access article under the: <https://creativecommons.org/licenses/by/4.0/>

INTRODUCTION

Building on past incidents, the phenomenon of infrastructure failure due to Lateral Spreading can result in significant loss of life and financial losses. This has occurred in various parts of the world, such as the Oakland Bay Bridge in San Francisco (1989), the Showa Bridge in Niigata, Japan (1964), the South Brighton Bridge in New Zealand (2011), and many more. These cases demonstrate similar conditions, such as events occurring along riverbanks, composed of alluvial soil containing loose sand, and locations experiencing strong shaking due to earthquakes. These three characteristics fulfill the criteria of the liquefaction phenomenon. The shaking increases pore water pressure, exerting pressure on the loose sandy soil particles, causing the soil to lose its strength and collapse.

These characteristics are also present in the regions of Indonesia. Seismically, Indonesia is located at the convergence of four active tectonic plates: the Australian Plate, the Eurasian Plate, the Philippine Plate, and the Pacific Plate. These plates undergo continental drift and cause geological disasters. Indonesia is known as the ring of fire, prone to earthquakes. The BMKG (Indonesian Meteorological, Climatological, and Geophysical Agency) states that Indonesia experiences at least 350 earthquakes with a magnitude of over five each year.

Earthquakes with a magnitude over five are destructive to buildings. Additionally, the characteristics of some buildings in Indonesia are located along river/coastal areas, with the soil composition being alluvial sandy soil.

The match between the characteristics of past infrastructure failure phenomena and the characteristics of infrastructure in Indonesia serves as a learning opportunity to understand the phenomenon of lateral spreading and take measures to prevent similar failures in the future. Therefore, understanding lateral spreading is the focus of this research.

METHOD

Analysis Data: Locations and Soil Investigation

Christchurch, the second largest city on New Zealand's South Island and a crucial regional economic center, is situated on the Canterbury Plains. These plains are composed of complex, layered soils deposited by rivers flowing eastward from the Southern Alps to the Pacific Ocean. In Christchurch, post-glacial surface sediments range in thickness from 15 to 40 meters, overlaying a sequence of gravel formations that are 300 to 500 meters thick, interspersed with layers of sand, silt, clay, and peat. These interlayered gravel and fine-grained soils form an artesian groundwater system with high water pressure. The shallow soil formations consist of alluvial gravel, sand, and silt (the Springston formation, dominating western Christchurch) or estuarine, lagoonal, dune, and swamp deposits of sand, silt, clay, and peat (the Christchurch formation, dominating the eastern suburbs) [1].

Soil investigation such as SPT has been conducted at several survey points and has been published on the official website of New Zealand, making soil data easily accessible. The following is the distribution of soil data points at several locations.

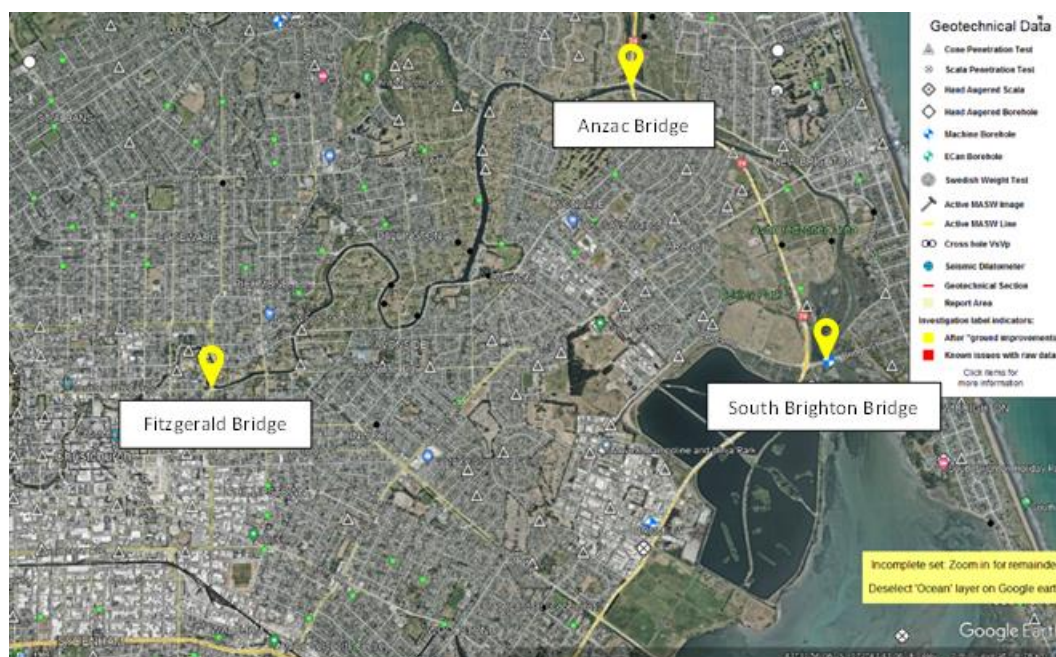


Figure 1. Distribution of Soil Investigation Points in Christchurch, New Zealand [2]

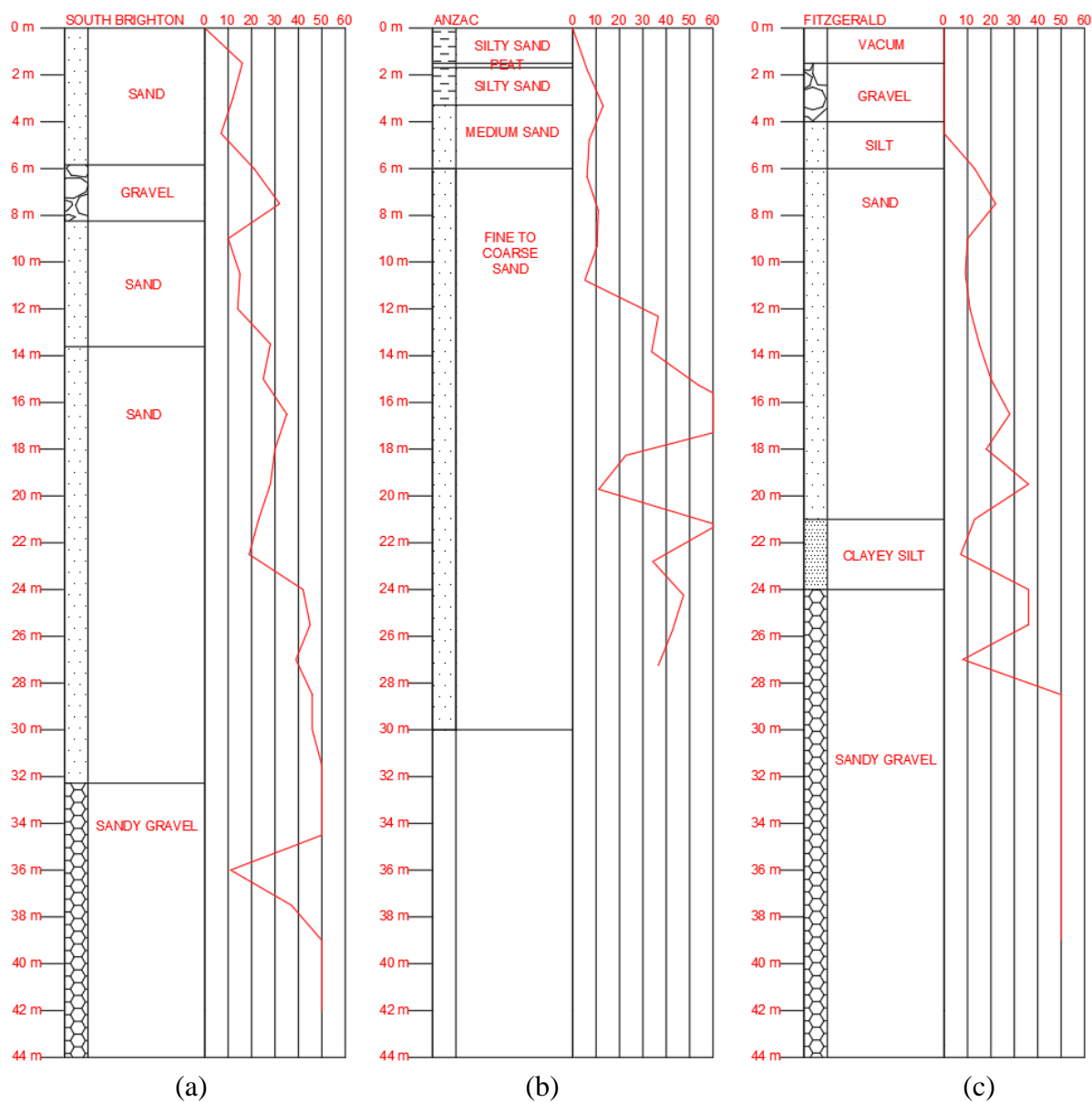


Figure 2. Soil Investigation (a) South Brighton Bridge [2], (b) ANZAC Bridge [1], and (c) Fitzgerald Bridge [2]

Analysis Data: Earthquake Data

The city of Christchurch has a high level of seismic activity. In the period from 2010 to 2011, there were at least 6 earthquakes [1]. Figure 3 shows the seismic data from that period

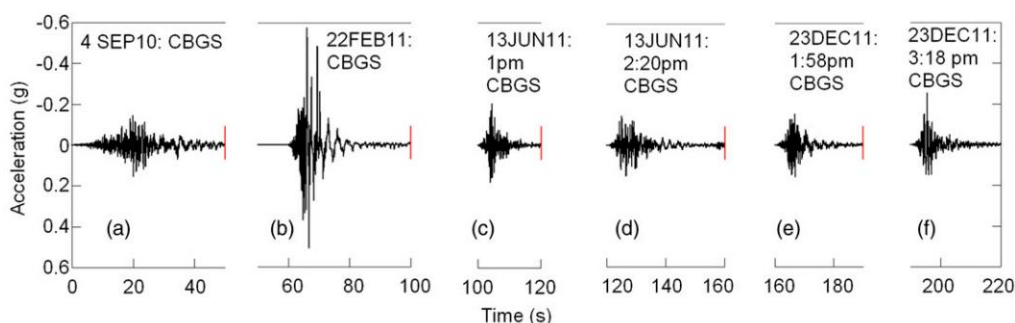


Figure 3. Recording of acceleration time histories at CBGS Christchurch during 6 earthquakes from September 4, 2010, to December 23, 2011[1]

In this study, the damage caused by lateral spreading occurred due to the Christchurch earthquake on February 22, 2011. Based on several recording stations, the Christchurch earthquake on February 22, 2011, had a horizontal PGA of 0.37g – 0.52g and a PGV of 30-90cm/s [2].

Empirical Method Analysis of Liquefaction: Boulanger and Idriss (2014)

The Idriss and Boulanger (2014) method provides a detailed framework for evaluating the potential for liquefaction during seismic events. This method incorporates the calculation of the cyclic stress ratio (CSR) and the cyclic resistance ratio (CRR) to determine the factor of safety (FS) against liquefaction. The equations used in this method are shown below:

Cyclic Stress Ratio (CSR)

$$CSR = \frac{0.65 \left(\frac{a_{max}}{g} \right) \sigma_v r_d}{\sigma_v'} \quad (1)$$

$$r_d = \exp(\alpha(z) + \beta(z)M) \quad (2)$$

$$\alpha(z) = -1.012 - 1.126 \sin\left(\frac{z}{11.73} + 5.133\right) \quad (3)$$

$$\beta(z) = 0.106 + 0.118 \sin\left(\frac{z}{11.28} + 5.142\right) \quad (4)$$

- σ_v = total overburden stress
- σ_v' = effective overburden stress
- a_{max} = peak horizontal acceleration at the ground surface
- g = acceleration due to gravity
- r_d = depth reduction factor to account for the flexibility of the soil column
- z = depth in meter
- M = Magnitude Earthquake

Cyclic Resistance Ratio (CRR)

$$CRR_{M, \sigma_v'} = CRR_{M=7.5, \sigma_v'=1} * MSF * K_\sigma \quad (5)$$

$$CRR_{M=7.5, \sigma'_v=1} = \exp\left(\frac{(N_1)_{60cs}}{14.1} + \left(\frac{(N_1)_{60cs}}{126}\right)^2 - \left(\frac{(N_1)_{60cs}}{23.6}\right)^3 + \left(\frac{(N_1)_{60cs}}{25.4}\right)^4 - 2.8\right) \quad (6)$$

$$MSF = 6.9 \exp\left(\frac{-M}{4}\right) - 0.058 \leq 1.8 \quad (7)$$

$$(N_1)_{60cs} = (N_1)_{60} + \Delta(N_1)_{60} \quad (8)$$

$$K_\sigma = 1 - \left(\frac{1}{18.9 - 2.55\sqrt{(N_1)_{60}}}\right) \ln \frac{\sigma'_v}{Pa} \leq 1.1 \quad (9)$$

$(N_1)_{60}$ for K_σ has limit ≤ 37

$$\Delta(N_1)_{60} = \exp\left(1.63 + \frac{9.7}{FC+0.01} - \left(\frac{15.7}{FC+0.01}\right)^2\right) \quad (10)$$

$$(N_1)_{60} = N_{60}C_N = (N_m C_E C_B C_R C_S)C_N \quad (11)$$

Table 1. SPT Correction [3]

Factor	Tools	Parameter	Correction
Overburden		CN	2.2/ (1.2+ σ_{vo} /Pa)
		CN	CN ≤ 1.7
Energy ratio	Donut hammer	CE	0.5 s.d 1.0
	Safety hammer	CE	0.7 s.d 1.2
	Automatic-trip Donut-type hammer	CE	0.8 s.d 1.3
Diameter Borehole	65 s.d 115 mm	CB	1.0
	150 mm	CB	1.05
	200 mm	CB	1.15
Rod length	< 3m	CR	0.75
	3 s.d 4 m	CR	0.8
	4 s.d 6 m	CR	0.85
	6 s.d 10 m	CR	0.95
	10 s.d 30 m	CR	1.0
Sampler	Split spoon w/o room for liners	CS	1.0
	Split spoon w/ room for liners	CS	1.1 s.d 1.3

MSF = Magnitude Scaling Factor

$(N_1)_{60}$ = eq. clean sand SPT

K_σ = Overburden correction

Pa = 1 atm = 100 kPa

Factor of Safety against Liquefaction

$$FS_{liq} = \frac{CRR}{CSR} \quad (12)$$

Liquefaction is expected to occur when the factor of safety against liquefaction (FS_{liq}) ≤ 1 [4].

Empirical Method Analysis of Lateral Spreading: Bartlett & Youd (2002) Method

The Bartlett and Youd (2002) lateral spreading analysis method is an extension of the methods developed by Bartlett and Youd (1992, 1995). The Bartlett and Youd method incorporate several factors including earthquake magnitude, horizontal distance to the earthquake source,

thickness of the liquefied layer, fines content, ground slope, and the ratio of the free-face height to the distance of the site [5].

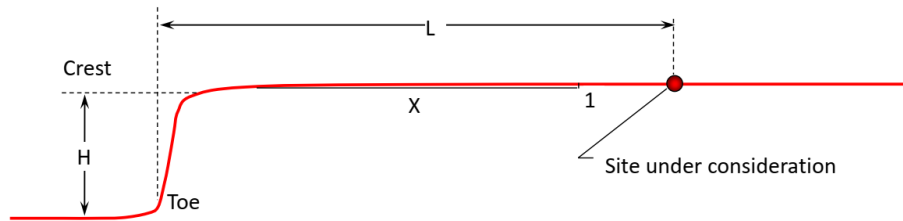


Figure 4. Bartlett & Youd (2002) Method

The equation for the free-face conditions model is:

$$\log D_H = -16.713 + 1.532M - 1.406 \log R^* - 0.012R + 0.592 \log W + 0.540 \log T_{15} + 3.413 \log(100 - F_{15}) - 0.795 \log(D50_{15} + 0.1mm) \quad (13)$$

For the mildly sloping ground model:

$$\log D_H = -16.213 + 1.532M - 1.406 \log R^* - 0.012R + 0.338 \log S + 0.540 \log T_{15} + 3.413 \log(100 - F_{15}) - 0.795 \log(D50_{15} + 0.1mm) \quad (14)$$

Where the values of R^* and R_0 are:

$$R^* = R + R_0 \quad (15)$$

$$R_0 = 10^{(0.89M - 5.64)} \quad (16)$$

The limitations of the Bartlett & Youd (2002) analysis are as follows:

Table 2. The limitations of the Bartlett & Youd (2002) analysis

Input Factor	Range of Values in Case History Database
Magnitude	$6.0 < M < 8.0$
Free-Face Ratio	$1.0\% < W < 20\%$
Ground Slope	$0.1\% < S < 6\%$
Thickness of Loose Layer	$0.3m < T_{15} < 12m$
Fines Content	$0\% < F_{15} < 50\%$
Mean Grain Size	$0.1mm < D50_{15} < 1mm$
Depth to Bottom of Section	Depth to Bottom of Liquefied zone $< 15m$

Empirical Method Analysis of Lateral Spreading: Byrne (1990) Method

The Byrne method for predicting deformation due to liquefaction is based on modeling an infinite slope with a uniform crust thickness and a liquefied layer acting as a resisting block on the inclined plane, as illustrated in the following figure 5. The Byrne (1990) method adopts mass M and spring KL as the strength and stiffness of the liquefied layer. The response of the liquefied layer is assumed to be linear elastic-plastic.

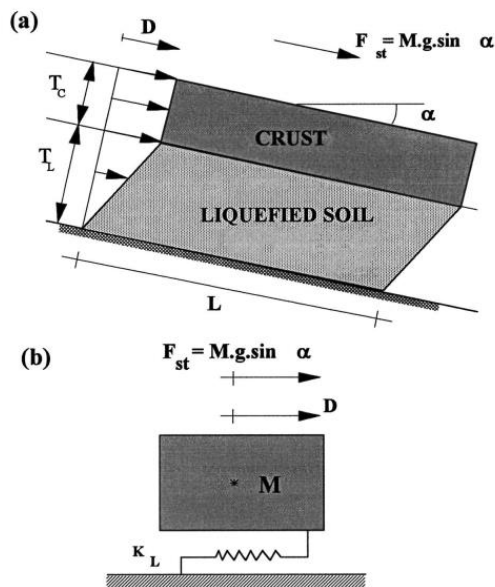


Figure 5. Model 1D Byrne (a) Idealized infinite slope (b) model [6]

The equation for estimating deformation due to liquefaction in soil based on Byrne's (1990) theory for linear stress-strain is as follows.

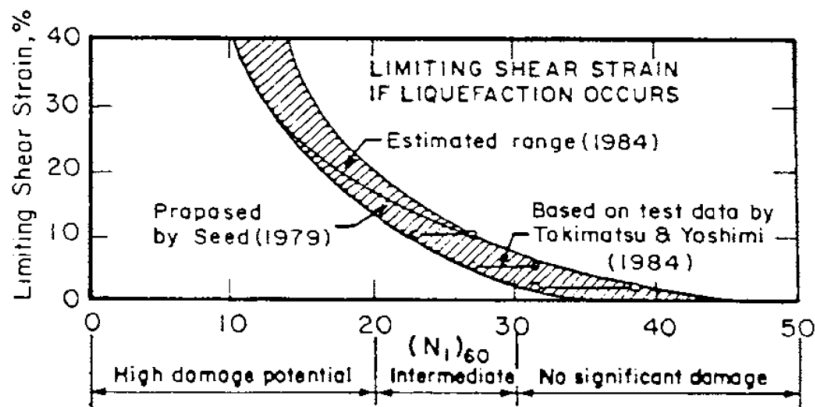


Figure 6. Relationship Between Limiting Shear Strain and $(N_1)_{60}$ Blow count [6]

Limiting strain, γ_{Lim} , are shown in Figure 6 based on laboratory tests from Seed et al. (1984). The range and average values of residual strength, S_r , and the limit strain, γ_{Lim} , from figure 6 are given in table 3.

Table 3. The range and average values of residual strength, S_r , and limit strain, γ_{lim} [6]

$(N_1)_{60}$	Sr Range Psf	Sr Avg. Psf	γ_{Lim} % Range	γ_{Lim} % Avg.
4	0-240	120	> 40	100
6	0-320	160	> 40	80
8	30-430	230	> 40	63
10	120-500	310	40-Large	50
12	200-680	440	32-Large	40
16	550-1100	825	20-30	25
20	> 2000	> 2000	13-20	16
30	> 2000	> 2000	3-7	5
40	> 2000	> 2000	0-3	1.5
50	> 2000	> 2000	0	0

The average s_r and γ_{Lim} values can be approximated by:

$$S_r = 3(N_1)_{60}^2 \frac{2000}{P_a} \quad (17)$$

P_a = the atmospheric pressure

$$\gamma_{LIM} = 10^{(2.2-0.5(N_1)_{60})} \quad (18)$$

Test data from Vaid (1990) suggests that the residual strength of very loose rounded sand under simple shear conditions is unlikely to be less than:

$$S_r = 0.087 \sigma'_{vo} \quad (19)$$

The soil mass, M , is given by:

$$M = (T_c \gamma_c + \frac{1}{2} T_L \gamma_L) / g \quad (20)$$

T_c and T_L are the thickness of the crust and liquefaction layers respectively, γ_c and γ_L are their respective unit weights, and g is the acceleration of gravity.

The driving stress, τ_{st} is given by:

$$\tau_{st} = (T_c \gamma_c + \frac{1}{2} T_L \gamma_L) \sin \theta \quad (21)$$

θ is the surface slope.

The spring stiffness, K_L , depends on the shear modulus of the liquefied soil, G_L , which in turn depends on the residual strength, s_r , and the limit displacement, γ_{Lim} , as follows:

$$G_L = S_r / \gamma_{LIM} \quad (22)$$

and the spring stiffness, K_L , is given by:

$$K_L = G_L / T_L \quad (23)$$

The displacement of the crust, D_{st} , due to the static driving stress applied to the softened liquefied layer is given by:

$$D_{st} = \tau_{st}/K_L \quad (24)$$

the change in kinetic energy as the velocity decreases from V_0 to zero results in the following equation for D_{dy} :

$$\text{For } D_{dy} < (D_{Lim} - D_{st}): \quad D_{dy} = \left[\frac{M}{K_L} V_0^2 + D_{st}^2 \right]^{1/2} \quad (25)$$

$$\text{For } D_{dy} > (D_{Lim} - D_{st}): \quad D_{dy} = \frac{1}{2} \left[D_{LIM} - D_{st} + \frac{D_{st}^2 + \frac{MV_0^2}{K_L}}{D_{LIM} - D_{st}} \right] \quad (26)$$

Where,

$$D_{LIM} = \gamma_{LIM} * T_L \quad (27)$$

The total displacement, D , is given by:

$$D = D_{st} * D_{dy} \quad (28)$$

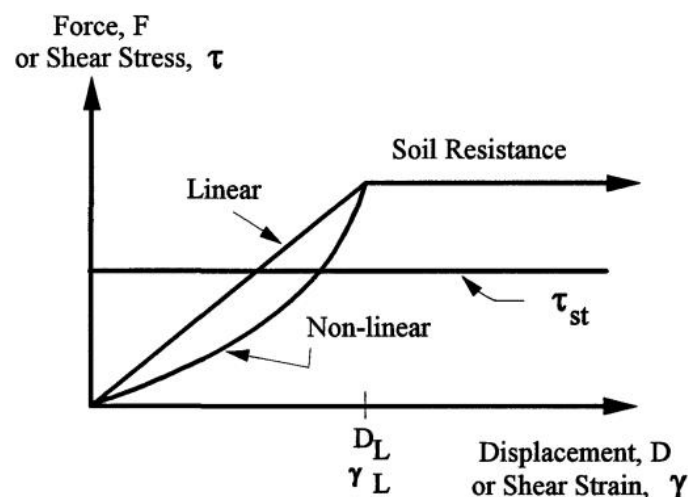


Figure 7. Linear dan Non-linear stress-strain models [6]

- D = displacement due to liquefaction
- D_{st} = static displacement
- D_L = displacement where soil resistance equals residual strength and is constant with increasing displacement
- K_L = stiffness of liquefied soil
- M = mass of soil
- V = velocity of the soil mass
- τ_{st} = initial static shear stress
- γ_L = shear strain limit or strain at residual strength
- S_r = average strength along the failure surface after liquefaction

RESULTS AND DISCUSSION

Liquefaction Susceptibility

The susceptibility to liquefaction in the case study of Christchurch can be analyzed from two main aspects. First, by examining the geological conditions of the location, as discussed in the sub-chapter on soil data. Below is a summary of liquefaction susceptibility based on the type and age of soil deposits.

Table 4. Summary of liquefaction susceptibility based on the type and age of soil deposits [7]

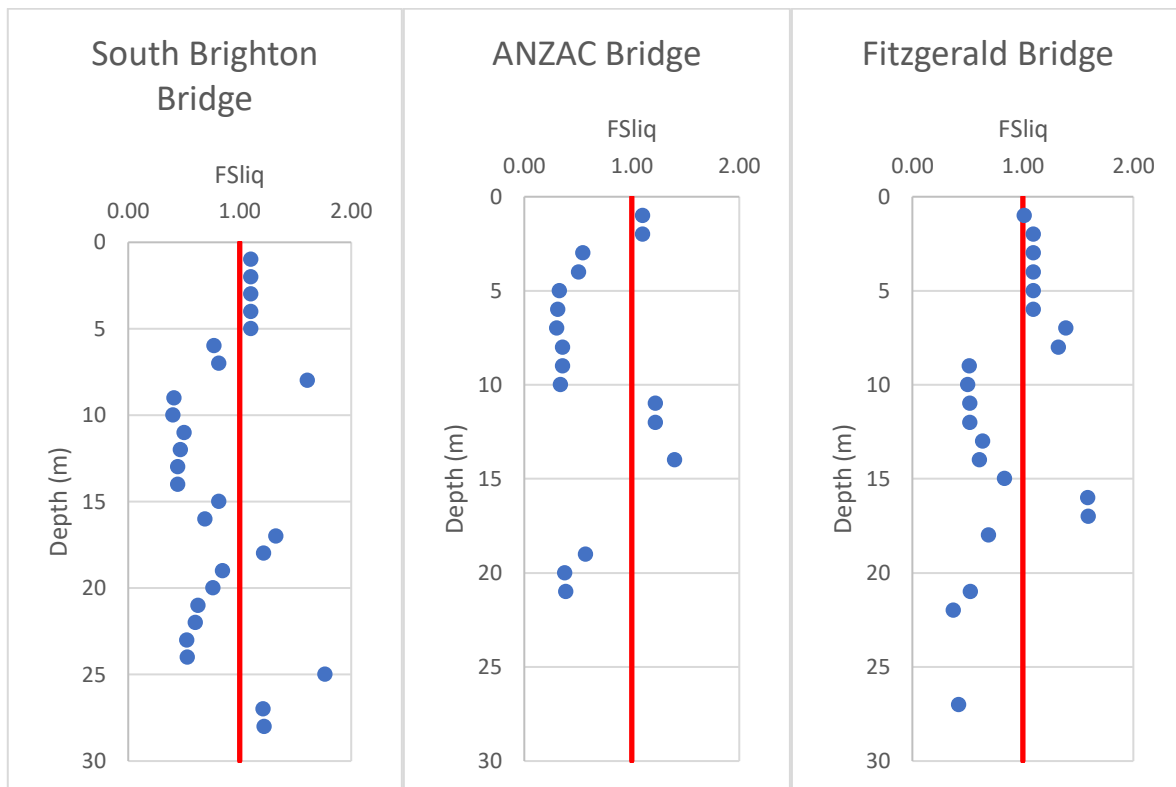
Type of deposit (1)	General distribution of cohesionless sediments in deposits (2)	Likelihood that Cohesionless Sediments, When Saturated, Would Be Susceptible to Liquefaction (by Age of Deposit)			
		<500 yr (3)	Holocene (4)	Pleis-tocene (5)	Pre pleis-tocene (6)
(a) Continental Deposits					
River channel Flood plain	Locally variable Locally variable	Very high High	High Moderate	Low Low	Very low Very low
Alluvial fan and plain	Widespread	Moderate	Low	Low	Very low
Marine terraces and plains	Widespread	-	Low	Very low	Very low
Delta and fan- delta	Widespread	High	Moderate	Low	Very low
Lacustrine and playa	Variable	High	Moderate	Low	Very low
Colluvium	Variable	High	Moderate	Low	Very low
Talus	Widespread	Low	Low	Very low	Very low
Dunes	Widespread	High	Moderate	Low	Very low
Loess	Variable	High	High	High	Unknown
Glacial till	Variable	Low	Low	Very low	Very low
Tuff	Rare	Low	Low	Very low	Very low
Tephra	Widespread	High	High	?	?
Residual soils	Rare	Low	Low	Very low	Very low
Sebeka	Locally variable	High	Moderate	Low	Very low

Table 5. Summary of liquefaction susceptibility based on the type and age of soil deposits [7]

Type of deposit (1)	General distribution of cohesionless sediments in deposits (2)	Likelihood that Cohesionless Sediments, When Saturated, Would Be Susceptible to Liquefaction (by Age of Deposit)			
		<500 yr (3)	Holocene (4)	Pleis-tocene (5)	Pre pleis-tocene (6)
(b) Coastal Zone					
Delta	Widespread	Very high	High	Low	Very low
Estuarine	Locally variable	High	Moderate	Low	Very low
Beach					
High wave energy	Widespread	Moderate	Low	Very low	Very low
Low wave energy	Widespread	High	Moderate	Low	Very low
Lagoonal	Locally variable	High	Moderate	Low	Very low
Fore shore	Locally variable	High	Moderate	Low	Very low
(c) Artificial					
Uncompacted fill	Variable Variable	Very high	--	--	--
Compacted fill		Low			

Based on the table 4 and table 5, it is evident that the soil formation layers in Christchurch, such as alluvial gravel, sand, and silt (Springston formation, predominantly in western Christchurch), or estuarine, lagoonal, dune, and marsh deposits consisting of sand, silt, clay, and peat, exhibit high susceptibility to liquefaction.

Secondly, the next aspect of liquefaction susceptibility is based on the Idriss and Boulanger (2014) equations. Based on the equations described in the sub-chapter on the Idriss and Boulanger (2014) liquefaction analysis method, figure 8 presents the analysis results.



(a) (b) (c)
Figure 8. Fslmq vs Depth of (a) South Brighton Bridge (b) ANZAC Bridge (c) Fitzgerald Bridge

Based on the analysis results shown in Figure 8 above, it indicates that each location experienced liquefaction, and liquefaction occurred below the surface soil layer. The failure of liquefaction in the lower layers can cause the spreading movement of soil on the surface. This characteristic or indication is a sign of lateral spreading. Thus, it can be understood that lateral spreading is one of the impacts of liquefaction that occurs when the subsurface layer experiences liquefaction, causing the soil above it to deform.

Lateral Spreading Analysis using Bartlett & Youd (2002) Method

Based on the equations described in the sub-chapter on the Bartlett & Youd (2002) lateral spreading analysis method, table 6 presents the analysis results.

Table 6. Lateral Spreading (Dh) Analysis Result of Bartlett & Youd (2002) Method

	M	R*(m)	R (m)	W	T15	F15	D50₁₅	Dh (m)
South Brighton Bridge	6.2	4.8	4.1	15	12	0.00	0.1	2.72
ANZAC Bridge	6.2	8.0	7.3	10	12	0.00	0.1	0.96
Fitzgerald Bridge	6.2	8.9	8.1	20	9	0	0.1	1.05

Lateral Spreading Analysis using Byrne (1990) Method

Based on the equations described in the sub-chapter on the Byrne (1990) lateral spreading analysis method, table 7 presents the analysis results.

Table 7. Lateral Spreading (D) Analysis Result of Byrne (1990) Method

	South Brighton Bridge	ANZAC Bridge	Fitzgerald Bridge
(N1)60	15	12	12
Pa (p`)	2116	2116	2116
Sr (psf)	825	680	696
Sr (kPa)	39	33	33
γ Lim (%)	20	32	32
TC (m)	4	2	3
TL (m)	16	11	11
γ C (kN/m3)	18	18	17
γ L (kN/m3)	18	18	17
γ (m/s2)	9.81	9.81	9.81
GL	1.97	1.02	1.04
M (kN/m3)	8.95	4.24	5.78
θ (°)	0.01	0.01	0.01
τ_{st} (kN/m3)	0.04	0.02	0.03
KL	0.12	0.09	0.09
Dst	0.31	0.25	0.27
V0	0.30	0.10	0.10
Dlim (m)	3.20	3.52	3.52
Ddy (m) Ddy<(Dlim-Dst)	2.57	0.72	0.83
Ddy (m) Ddy> (Dlim-Dst)	0.55	0.17	0.19
D (m)	2.88	0.98	1.09

Discussion Summary of Analysis Results

The following is a summary of the deformation magnitude due to lateral spreading using the methods of Bartlett & Youd (2002) and Byrne (1990). The results of these analyses are then compared with the lateral spreading measurements obtained from field surveys and aerial LiDAR observations.

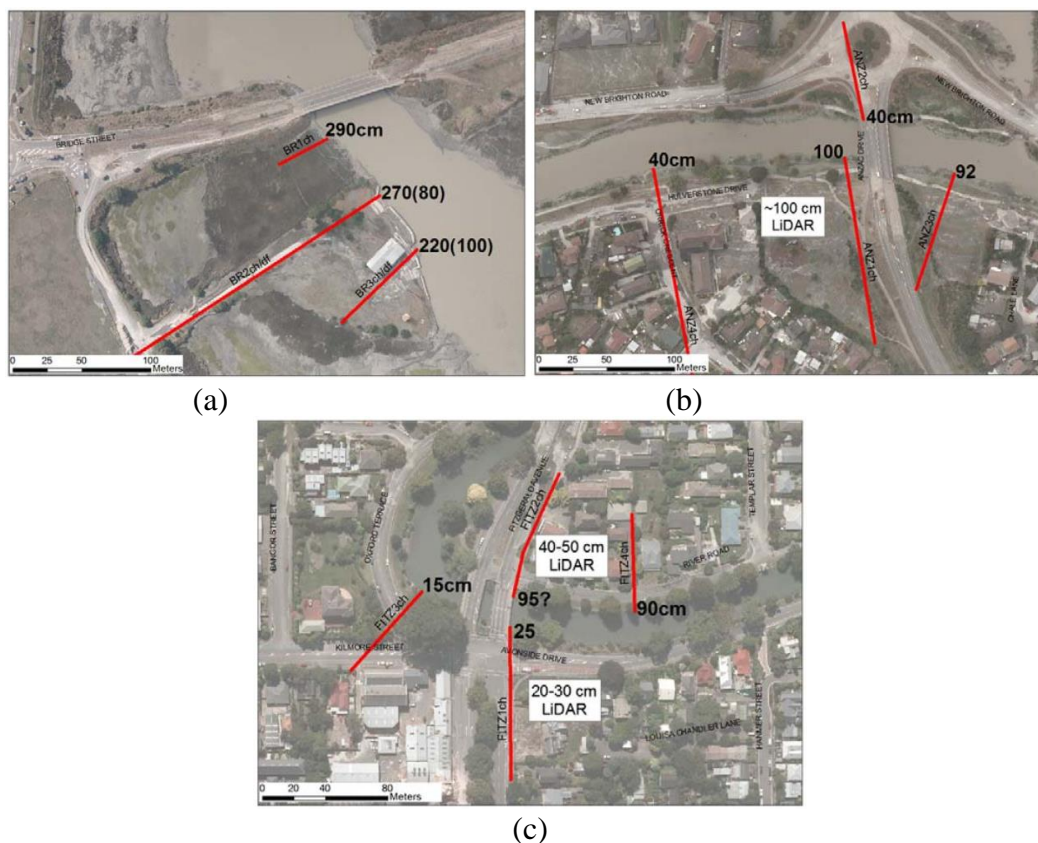


Figure 9. Aerial Cross-Section Images Results from the ground survey LIDAR for: (a) South Brighton Bridge, (b) Anzac Bridge, and (c) Fitzgerald Bridge [1]

Table 8. Summary of Analysis Results Compared with Observations

Lokasi	D (m)		
	Bartlett & Youd (2002)	Byrne (1990)	Lidar
South Brighton Bridge	2.72	2.88	2.9
ANZAC Bridge	0.96	0.98	1
Fitzgerald Bridge	1.05	1.09	0.95

The results of the deformation analysis due to lateral spreading using the Bartlett & Youd (2002) method and the Byrne (1990) method were compared with field measurements and aerial LiDAR observations. This comparison reveals several consistencies and discrepancies. Here is a summary of the comparison:

Bartlett & Youd (2002) Method:

1. The analysis results show reasonably accurate predictions of lateral spreading deformation at several locations.
2. Locations such as ANZAC Bridge show good agreement between the analysis results and field observations.
3. However, at other locations like South Brighton Bridge and Fitzgerald Bridge, there are slight discrepancies between the analysis results and field observations, possibly due to the variability of local soil conditions.

Byrne (1990) Method:

1. This method also provides accurate predictions of deformation due to lateral spreading at several locations.
2. The analysis results at ANZAC Bridge show good agreement with the aerial LiDAR observations.
3. Some locations show minor differences in deformation predictions, which may be due to the assumptions in the Byrne model not fully reflecting actual soil conditions.

Field Observations and Aerial LiDAR:

1. Field observations and aerial LiDAR data provide a clear picture of the deformation occurring due to lateral spreading.
2. This data is crucial for comparing and validating the analysis results from both methods.
3. Field measurements and aerial LiDAR data generally show deformation occurring in the subsurface layers affecting surface soil movement, consistent with the characteristics of lateral spreading.

CONCLUSION

From the results of the analysis conducted, it can be concluded that both analytical methods, Bartlett & Youd (2002) and Byrne (1990), show good agreement with field observations and aerial LiDAR data. This indicates that lateral spreading, as an impact of liquefaction, can be well predicted using these methods. However, the variability of local soil conditions should be considered in the analysis for more accurate results.

There are some recommendations for the future research:

Expand the Scope of Modeling:

It is recommended that the modeling be extended beyond the three locations analyzed in this study. Additional locations should be included to improve the accuracy and reliability of the results.

1. Utilize Updated Methods:

The analysis should also consider utilizing more updated methods if available. Incorporating numerical calculations is advisable to enhance the robustness of the analysis.

2. Review Potential for Lateral Spreading:

According to the SNI geotechnical design standards, it is crucial to review the potential for lateral spreading when liquefiable layers are present, especially for constructions located in or near water bodies such as bridges, wharf, etc.

By considering these recommendations, future studies can provide more comprehensive insights and improve the applicability of the findings to geotechnical engineering practices.

REFERENCE

- [1] M. Cubrinovski, J. Haskell, A. Winkley, K. Robinson and L. Wotherspoon, "Performance of Bridges in Liquefied Deposits during the 2010–2011 Christchurch, New Zealand, Earthquakes," *JOURNAL OF PERFORMANCE OF CONSTRUCTED FACILITIES*, pp. 24-39, 2014.
- [2] "Investigation Logs," CGD (Canterbury Geotechnical Database), 2012. [Online]. Available: <https://www.nzgd.org.nz/>. [Accessed 1 January 2024].

-
- [3] SNI 4135:2008, Badan Standardisasi Nasional, 2008.
- [4] J. D. B. J. M. R. L. Christopher S. Markham, "Evaluating nonlinear effective stress site response analyses using," *Soil Dynamics and Earthquake Engineering*, vol. 82, no. Soil Dynamics and Earthquake Engineering, pp. 84-98, 2015.
- [5] C. M. H. a. S. F. B. T. Leslie Youd, "Revised Multilinear Regression Equations for Prediction," *JOURNAL OF GEOTECHNICAL AND GEOENVIRONMENTAL ENGINEERING*, pp. 1007-1017, 2002.
- [6] P. M. Byrne, "A Model for Predicting Liquefaction Induced Displacement," in *1991 - Second International Conference on Recent Advances in Geotechnical Earthquake Engineering & Soil Dynamics*, University of British Columbia, Vancouver, B.C., Canada, 1991.
- [7] D. M. P. T. Leslie Youd, "Mapping Liquefaction-Induced Ground Failure Potential," *Journal of Geotechnical Engineering Division*, pp. 433-446, 1978.